The Critical Role of Temperature-dependent Mobilities in Determining the Open-Circuit Voltage of Bulk-heterojunction Organic Solar Cells

Yahui Tang,[1,2,a)] Girish Lakhwani,[2] and Christopher R. McNeill [1]

[1]*Department of Materials Science and Engineering, Monash University, Victoria 3800, Australia*

[2]*ARC Centre of Excellence in Exciton Science, School of Chemistry, The University of Sydney, Camperdown, NSW*

2006, Australia

While solution-processed bulk-heterojunction organic solar cells (OSCs) continue to attract attention as their efficiencies approach 20%, the physical origin of the non-radiative energy loss in OSCs remains under debate. Understanding the temperature dependence of open-circuit voltage (V_{OC}) is thus important because it provides unique insights into the origin of energy loss. Herein, we simulate the V_{OC} vs. T relation of PTB7-Th:PC$_{71}$BM bulk-heterojunction OSCs within the range of 160–295 K by incorporating experimentally measured temperature-dependent mobilities into the drift-diffusion model, assuming bimolecular recombination as the primary recombination mechanism. Significantly, we find that the temperature dependence of V_{OC} can only be correctly reproduced by the model when the temperature dependence of the carrier mobilities is taken into account. The effect of the Langevin reduction coefficient on the temperature dependence of V_{OC} is also investigated.

[a)] Electronic mail: yahui.tang@sydney.edu.au

Organic solar cells (OSCs) continue to attract interest with power conversion efficiencies approaching 20% increasing their viability for commercialization.[1,2] While recent efficiency improvement is encouraging, the physical origin of the open-circuit voltage (V_{OC}) loss and the maximum achievable V_{OC} is still under debate. One of the areas yet to be fully understood is the temperature dependence of V_{OC}.[3–8] Temperature is a key parameter associated with many important processes in a bulk heterojunction (BHJ) solar cell, such as charge transport and recombination. Getting an accurate description of the temperature dependence of V_{OC} is especially important since it is related to the physical origin of nonradiative loss. [9,10] This is because the non-radiative loss in OSCs, which is the energy lost through nonradiative pathways, is closely related to thermally activated processes and is thus temperature dependent. Understanding the temperature dependence of V_{OC} is also of practical interest because the extrapolation of V_{OC} vs. T curves to 0 K is often used to estimate the maximum achievable V_{OC} or the charge transfer state energy (E_{CT}) since the bimolecular recombination is expected to vanish with the temperature approaching 0 K.

Indeed, as experimentally observed by Vandewal et al., the linear extrapolation of the V_{OC} vs. T curve and the E_{CT} vs. T curve to 0 K was found to result in the same value, providing an intrinsic limit to the maximum achievable V_{OC} of OSCs.[8] However, it has also been shown that the V_{OC} vs. T curve undergoes a drastic turnover at low temperatures for some donor:acceptor BHJ devices, which questions the validity of linear extrapolation of V_{OC} to 0 K. Such a V_{OC} drop was first attributed to entropy-driven charge generation, which decreases at low temperatures.[7] Another proposed physical origin is that the Gaussian density of states effectively alters the molecular energy levels and replaces the effective bandgap E_g with $\left(E_g - \frac{\sigma_n^2 + \sigma_p^2}{2kT}\right)$,[4,11] which can lead to a drastic V_{OC} drop at low temperatures. While these two explanations are not in favor of the linear description of the V_{OC} vs. T relation, it is also argued that the temperature dependence of V_{OC} can be affected by high leakage current that competes with the photocurrent and becomes significant enough to decrease V_{OC} at low temperatures.[6,12,13] This suggests that V_{OC} turnover at low temperatures does not originate from the intrinsic properties of the BHJ layer materials. Furthermore,

the V_{OC} vs. T relationship may also show nonlinear saturation at low temperatures subject to the energetic barriers at the contacts,[14,15] which also does not originate from the intrinsic properties of BHJ layers. The coherent agreement of experimental measurement and numerical simulation is yet to be obtained for the temperature-dependent V_{OC} of BHJ organic solar cells. Therefore, this paper studied the physical origin of the temperature-dependent V_{OC} using PTB7-Th:PC$_{71}$BM as a model system, combining experimental measurement and numerical simulations.

The influence of temperature on V_{OC} is complicated by multiple factors, and one of the most important factors is the temperature-dependent recombination rate,[16] since it changes the product of electron and hole densities (np) and thus the quasi-Fermi level splitting. For PTB7-Th:PC$_{71}$BM BHJ devices processed with the additive DIO, trap-assisted recombination is largely suppressed,[17] leaving bimolecular recombination as the main recombination mechanism. The bimolecular recombination rate in OSCs is given by,[18,19]

$$R = \frac{\eta(\mu_n + \mu_p)q}{2\varepsilon}(np - n_i^2) \tag{1}$$

where η is the Langevin reduction coefficient, μ_p/μ_n are the mobilities of holes/electrons, n/p is the charge carrier densities of electrons and holes, n_i is the intrinsic charge carrier density, q is the elementary charge, and ε is the dielectric constant. Based on Equation 1, temperature-dependent mobilities will lead to a temperature-dependent recombination rate, which may consequently impact the low-temperature V_{OC} of OSCs. The Langevin reduction coefficient η also affects the recombination rate and subsequently affects the V_{OC} vs. T relation, but it is not likely to be temperature dependent since it is a property related to the BHJ morphology.[20,21]

To study the influence of temperature-dependent mobilities and the Langevin reduction coefficient on the V_{OC} vs. T relation, we first measured the temperature-dependent mobilities using the space charge-limited current (SCLC) method. We measured current density-voltage (JV) curves of electron- and hole-

only devices with PTB7-Th:PC_{71}BM as the BHJ layer at temperatures between 200-295 K and obtained the temperature-dependent mobilities by fitting the SCLC JV curves into the extended Mott-Gurney square law.[22,23] The extracted temperature-dependent mobilities were fitted using an Arrhenius relation, and then used in the drift-diffusion simulation of the V_{OC} vs. T curve. We estimated the Langevin reduction coefficient by fitting the room-temperature JV curve of inverted BHJ PTB7-Th:PC_{71}BM solar cell devices with a drift-diffusion model, assuming bimolecular recombination to be the only recombination mechanism. After obtaining the Langevin reduction coefficient and the temperature-dependent mobilities, the V_{OC} vs. T curve was simulated using a drift-diffusion model, including the temperature-dependent mobilities implemented by a commercial software package (Setfos 5.2, Fluxim). In our simulations, we find that although the Langevin reduction coefficient has a noticeable influence on the V_{OC} vs. T curve, the experimental V_{OC} vs. T curve can only be reproduced when the temperature-dependent mobilities are included. This highlights the critical role of temperature-dependent mobilities in determining the temperature dependence of V_{OC}.

We start with the fabrication of single carrier devices for measuring the electron and hole mobilities at different temperatures. Hole-only devices and electron-only devices had a device architecture of ITO/PEDOT:PSS/Blend/MoO_3/Ag and ITO/PEDOT:PSS/Al/Blend/Ca/Al, respectively. The blend layer was comprised of PTB7-Th:PC_{71}BM of 1:1.5 ratio and processed using dichlorobenzene and 3 vol.% 1,8-diiodooctane as the solvent additive. More details about the fabrication and characterization are included in the supplementary information. The dark JV curves of the electron- and hole-only devices were measured at temperatures ranging between 200 K to 295 K with 20 K steps, with the obtained temperature-dependent SCLC JV curves and the fittings shown in Fig. 1.
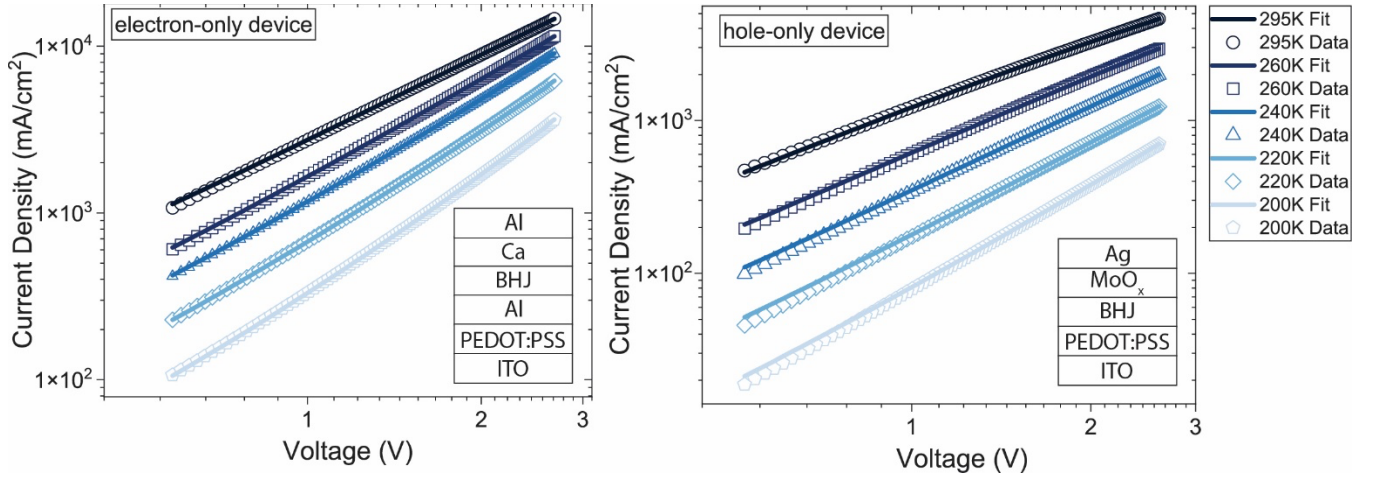
FIG. 1. Temperature-dependent current density-voltage characteristics of single carrier devices and fitting to Equation 2.

To describe the temperature-dependence of mobility, the extended Mott-Gurney quadratic equation, including a field enhancement factor γ introduced by Murgatroyd and Gill (MG) was used to fit the SCLC JV curves:[22,23]

$$J = \frac{9}{8}\varepsilon_r\varepsilon_0\mu_0\frac{(V-V_{bi})^2}{L^3}exp\left(0.891\gamma\sqrt{\frac{V-V_{bi}}{L}}\right) \tag{2}$$

in which μ_0 is the zero-field mobility, and γ is a field-enhancement factor. $\varepsilon_r\varepsilon_0$ is the dielectric constant of the blend layer with ε_r assumed to be 3.5 throughout the paper. V_{bi} is the built-in field originating from the electrode work function offset, and L is the thickness of the blend layer. The experimental data are all well-fitted using Equation 2 at all temperatures within the 200 K to 295 K range, as shown in Fig.1. The obtained temperature-dependent μ_0 and γ are plotted against $1/T$ in Fig.2(a) and (b). As shown in Fig.2, both μ_0 and γ are linearly dependent on $1/T$ within the temperature range of interest. The following analysis was applied to extract temperature-dependent parameters.
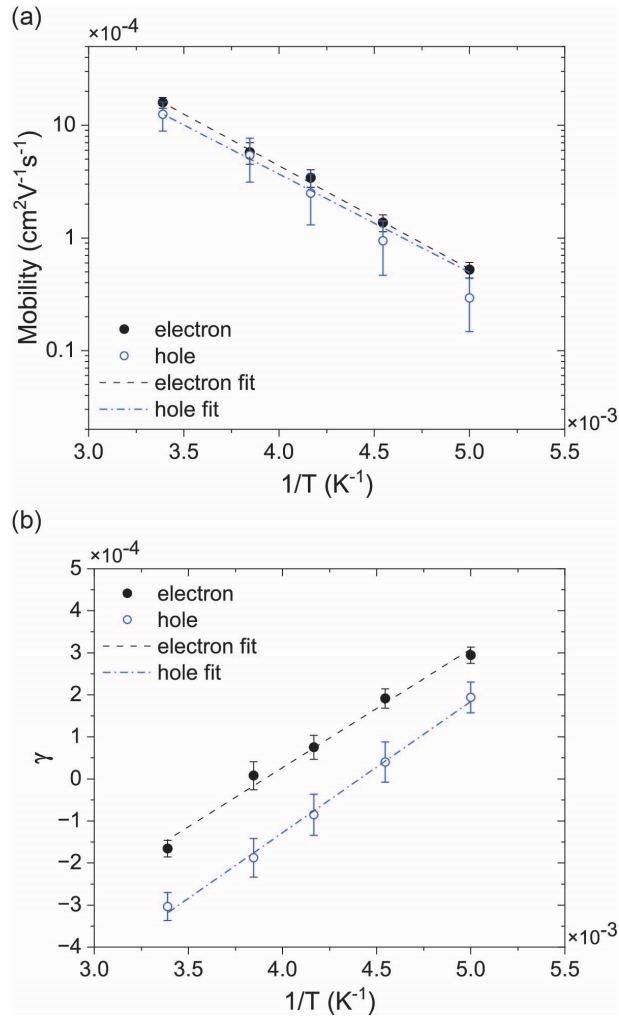
FIG. 2. (a) Temperature-dependent electron (μ_n) and hole mobility (μ_p) and fitting to Equation 3. (b) Temperature-dependent gamma and fitting to Equation 4. The values are averaged values of more than five independent devices, and the errors are standard deviation values of all measurements on different devices. All fitting parameters are summarized in Table I.

The temperature dependence of zero-field mobility is described by the following Arrhenius relation:[24]

$$\mu_0(T) = \mu_* exp\left(\frac{-E_a}{kT}\right) \tag{3}$$

where E_a is the activation energy, μ_* is the mobility at zero electric field and T→ ∞, k is the Boltzmann constant, and T is the temperature. Fitting of reasonable quality was achieved (within errors as determined by the standard deviation obtained from measuring and fitting multiple devices) as shown in Fig.2(a). The obtained E_a values are 0.18 and 0.17 eV for electrons and holes, respectively, which is very close to the values reported for the same donor:acceptor system.[25] The obtained values of μ_* are 2.0 ± 0.5 cm^2 V^{-1} s^{-1}

and 1.1 ± 0.4 cm^2 V^{-1} s^{-1} for electrons and holes, which are lower than the universal value 10 cm^2 V^{-1} s^{-1} observed for disordered organic semiconducting materials,[24] which is probably due to the fact that we measured BHJ devices here while the universal value was measured for devices comprised of neat materials. The field dependence $\gamma(T)$ is then fitted to an empirical temperature-dependent expression firstly used by Gill:[26]

$$\gamma(T) = B\left[\frac{1}{kT} - \frac{1}{kT_0}\right] \tag{4}$$

in which B and T_0 are two constant coefficients, with B representing the slope of γ vs. $1/T$ and T_0 the temperature at which γ equals zero.[4] Reasonable accuracy has been achieved for the single carrier devices measured as shown in Fig.2(b), and the values obtained for B and T_0 are comparable to those obtained for other donor:acceptor BHJ devices reported in the reference.[25]

TABLE I. Fitting parameters obtained from fitting the temperature-dependent zero-field mobility and the field dependence factor.

Electron-only device		
E_a	0.18 ± 0.01	eV
μ_*	2.0 ± 0.5	cm^2 V^{-1} s^{-1}
B	$(3.8 \pm 0.2) \times 10^{-24}$	V cm$^{0.5}$ V$^{-0.5}$
T_0	256 ± 3	K
Hole-only device		
E_a	0.17 ± 0.01	eV
μ_*	1.1 ± 0.4	cm^2 V^{-1} s^{-1}
B	$(4.3 \pm 0.2) \times 10^{-24}$	V cm$^{0.5}$ V$^{-0.5}$
T_0	227 ± 1	K

Although Arrhenius-type relationships are used to describe the temperature-dependent mobility and temperature dependence of γ, it is noted that the Gaussian disorder model (GDM) and its extended variants are also widely used, in which the mobilities follow a $1/T^2$ temperature dependence.[27,28] Felekidis et al. recently investigated and analyzed the mobilities of a wide range of polymer:fullerene blends using both Arrhenius-type relations and GDM models. They found that the Arrhenius analysis leads to an accurate

description for most of the measured materials.[25] Moreover, theoretical modeling considering tens of parameters reflecting the chemistry of the materials recently conducted by Fornari et al. found that the steady-state charge mobilities in the low carrier density and low electric field limit depend only on the effective structural disorder and electron-phonon coupling.[29] Their results support the experimental observation of a universal Arrhenius thermally activated charge transport in diodes consisting of disordered organic semiconductors.[24] Because of the reasons above, we used the Arrhenius-type analysis for the temperature-dependent mobilities. A good agreement between data and fittings was achieved within the temperature of interest, as shown in Fig. 2.

After obtaining the temperature-field-dependent mobility parameters, we investigate the temperature dependence of the V_{OC} of the BHJ device, which has an inverted architecture of ITO/PEIE/BHJ/MoO$_3$(12nm)/Ag(100nm).[6] For the illumination of OSC devices in the cryostat, a Thorlabs MWWHL3 warm white mounted LED driven by a Thorlabs DC2100 LED driver was used for temperature-dependent light JV measurement. Light intensities were adjusted to produce a similar J_{SC} and V_{OC} to that under AM 1.5G illumination. The V_{OC} values were then extracted from temperature-dependent JVs and plotted against temperature, with the obtained V_{OC} vs. T relation shown as the solid red circles in Fig. 3(b).

Before simulating the temperature-dependence of V_{OC}, the Langevin reduction coefficient η is estimated by fitting the room-temperature JV curve to a drift-diffusion model, considering a constant mobility of 1.6×10^{-3} cm^{2}V^{-1}s^{-1} for electrons and 1.3×10^{-3} cm^{2}V^{-1}s^{-1} for holes, with both values obtained from the SCLC measurements at room temperature. $N_{0, HOMO}$, and $N_{0, LUMO}$ were set as 2×10^{25} m^{-3}, same as the values used for P3HT:PCBM in the reference.[30] The local value of η optimized by the Levenberg-Marquardt method in the commercial software Setfos, with a value of 0.03 obtained as the Langevin reduction coefficient. The obtained value is comparable to the values commonly used for donor:acceptor organic photovoltaics.[31] As shown in Fig.3(a), the fitted JV curve is in reasonable

8

agreement with the experimental data, with some discrepancy in current density observed around V_{OC}, leading to a higher fill factor in the simulation. Such a discrepancy is possibly due to trap-assisted recombination which can lead to a lower fill factor (but does not effectively change V_{OC}) that is not accounted for in the simulation. Although trap-assisted recombination exists, it is insignificant in PTB7-Th:PC$_{71}$BM processed with solvent additive DIO,[17] hence does not affect the V_{OC} vs. T relation in this system. The estimated value of η, together with the fitting parameters that describe the temperature-field-dependent mobilities used to simulate the temperature-dependent V_{OC}, are summarized in Table II. The probability of charge separation P is assumed to be constant at all temperatures. The assumption of constant charge photogeneration is supported by temperature independent charge photocarrier generation found in photophysical measurements for polymer:fullerene blends.[5] Simulations including the temperature-field-dependent mobilities, describes the V_{OC} vs. T relation well, as shown in Fig.3(b). In contrast, the discrepancy between the experimental data and the simulation using constant mobilities is significant, highlighting the critical role of the temperature dependence of mobilities in determining the V_{OC} vs. T relationship. We did not include the effect of shunt resistance or series resistance in our simulations since we found the simulation without the resistance can adequately reproduce the experimental results within the measured temperature range.

TABLE II. Drift-diffusion simulation parameters used in Setfos.

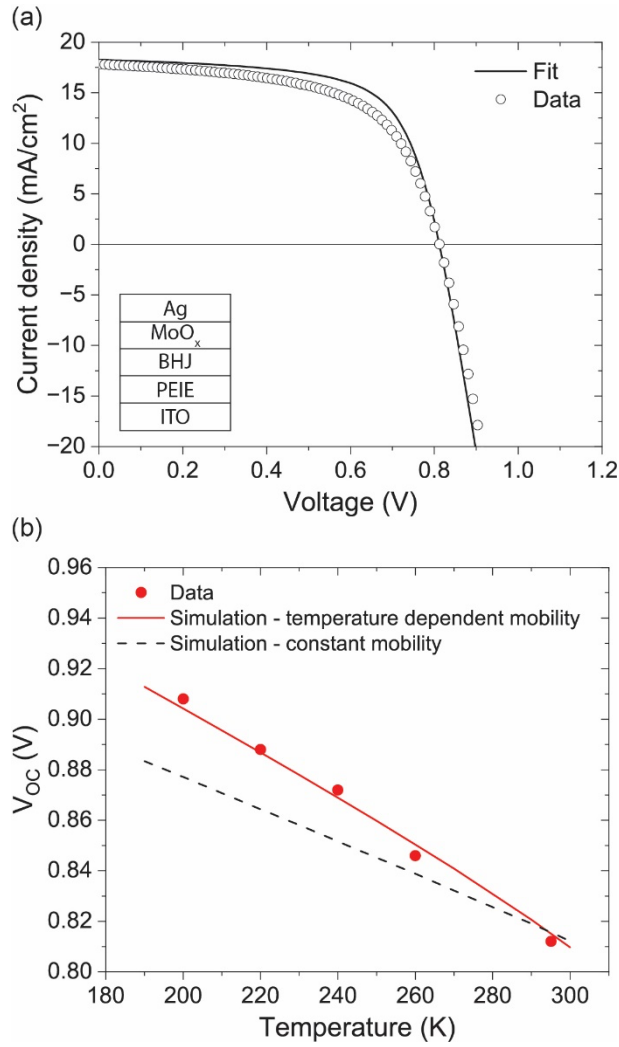| Simulation Parameters		
Optical generation efficiency	0.8	
Langevin reduction coefficient	0.03	
HOMO	5.2	eV
LUMO	3.9	eV
$N_{0,\,HOMO}$	2×10^{25}	m^{-3}
$N_{0,\,LUMO}$	2×10^{25}	m^{-3}
Active layer thickness	120	nm
μ_n at room temperature	1.6×10^{-3}	cm^{2}V^{-1}s^{-1}
μ_h at room temperature	1.3×10^{-3}	cm^{2}V^{-1}s^{-1}

FIG. 3 (a) Fitting of current-voltage characteristics measured under 1-sun conditions to the drift-diffusion model to extract the Langevin reduction coefficient. The obtained Langevin reduction coefficient is 0.03; (b) Measured temperature-dependent open-circuit voltage (symbols) and simulated temperature-dependent open-circuit voltage (lines) conducted with either constant (dashed line) or temperature-dependent (solid line) mobilities. The parameters used for the simulation with constant mobilities are presented in Table II. For the simulation with temperature-dependent mobilities, the mobility parameters used are extracted from experimental measurements as summarized in Table I, with the other parameters the same as the ones used for the simulation with constant mobilities. All the simulations are conducted using the commercial software Setfos.

While the fact that the V_{OC} vs. T relation cannot be simulated using constant mobilities suggests the critical role that temperature-dependent mobilities play in determining the V_{OC} vs. T relation, the Langevin reduction coefficient η may also affect the V_{OC} vs. T relation as indicated by Equation 1. Therefore, to further investigate the influence of Langevin reduction coefficient η, we simulated the V_{OC} vs. T relation
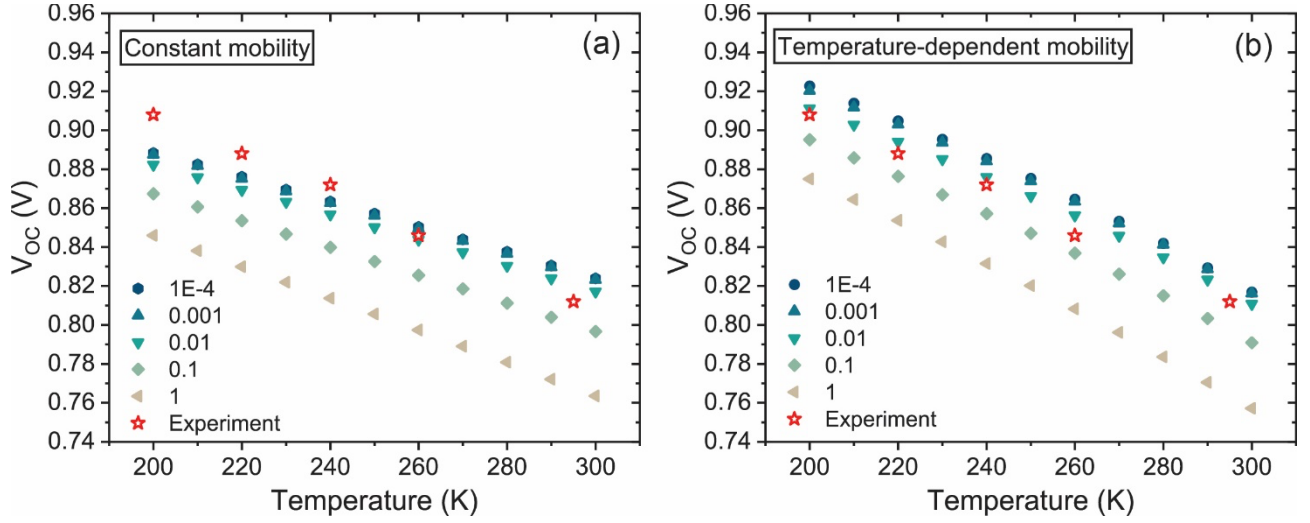
FIG. 4. Simulated temperature-dependent open-circuit voltage for different Langevin reduction coefficients with (a) constant mobilities given in Table II; (b) temperature-dependent mobilities presented in Table I. The experimentally measured V_{OC} vs. T data (stars) is plotted for comparison.

using varied η with both constant mobilities and temperature-dependent mobilities, as presented in Fig. 4(a) and (b), respectively. Comparing Fig. 4(a) and (b) highlights the critical role of temperature-dependent mobilities in determining the V_{OC} vs. T relation of solar cell devices. As shown in Fig. 4(a), although increasing η can lead to a steeper V_{OC} vs. T relation, even the simulation with an ideal Langevin recombination ($\eta = 1$) cannot reproduce the experimentally measured V_{OC} vs. T relation. In contrast, the simulation with temperature-dependent mobilities presented in Fig.4(b) shows that the V_{OC} vs. T relation is steeper than in Fig. 4(a). Also, the fact that the experimental data fall in between the simulations with Langevin reduction coefficients of 0.1 and 0.01 supports that 0.03 is indeed a reasonable estimation. Most importantly, Fig.4(b) suggests that although increasing η can lead to a larger V_{OC} vs. T slope, the contribution from the temperature-dependent mobilities is critical, and the experimental V_{OC} vs. T relation cannot be reproduced without considering temperature-dependent mobilities. Lower mobilities lead to a smaller reduced Langevin recombination rate as temperature decreases. Assuming a temperature-independent generation rate for the measured system,[5] a lower recombination rate consequently shifts the

generation-recombination kinetic balance and results in a higher open-circuit voltage than the values predicted by the constant mobility model.
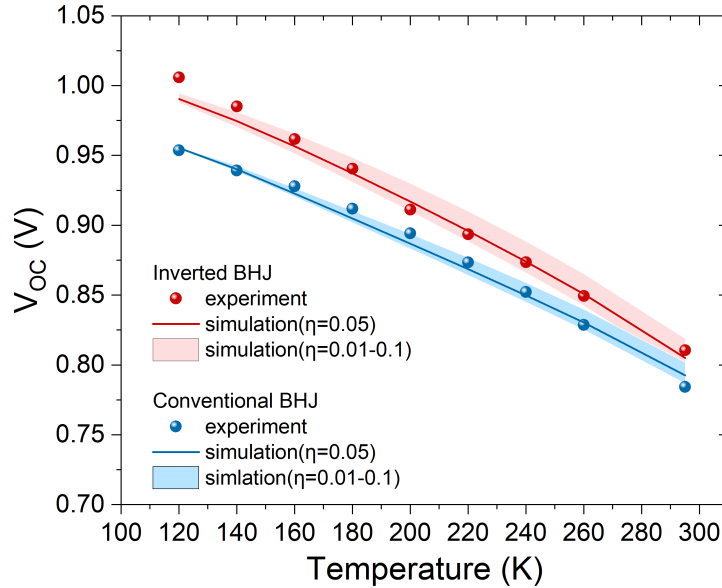

FIG.5. Validity test of the method with different device architectures within a wider temperature range.

To test the validity of this method at lower temperatures, mobilities between 120 K and 295 K were extracted using the previously described SCLC method, and the obtained parameters that describe the temperature-dependent mobilities were used for modeling the temperature-dependent V_{OC} within this range. Furthermore, conventional BHJ devices with the same active layer were fabricated and modeled using the same method (with the same set of parameters for temperature-dependent mobilities). The temperature-dependent mobility data and the details of fitting are shown in Fig.S3 and Table SI. Since the Langevin reduction coefficient η is an estimated parameter and may introduce deviations, values between 0.01-0.1 were used simulated and shown as the colored regions for comparison with the experimental data in Fig.5. Simulations with η = 0.01 are used as the lower boundary and simulations with η = 0.01 are used as the upper boundary for the colored regions in Fig.5. The simulations for two architectures with η=0.05 are also plotted as guides of eyes for readers. As shown in Fig.5, the model describes the data reasonably well at temperatures above 160 K for PTB7-Th:PC$_{71}$BM inverted and conventional BHJ devices. Other

physical mechanisms of charge recombination/transport mechanisms in the BHJ layer may exist at temperatures lower than 160 K or in other donor:acceptor systems,[32] and temperature-independent parameters assumed for this system can be temperature-dependent in other systems/at lower temperatures.[33] However, one should carefully make sure that V_{OC} measured at lower temperatures/for other materials are not limited by factors other than the BHJ charge transport/recombination processes by measuring devices of different architectures.

To conclude, we have simulated the V_{OC} vs. T relation of PTB7-Th:PC$_{71}$BM inverted BHJ solar cells between 160 and 295 K using experimentally measured temperature-dependent mobilities. To understand the effect of the Langevin reduction coefficient and temperature-dependent mobilities on the V_{OC} vs. T relation, we have additionally simulated the influence of varying the Langevin reduction coefficient with constant and temperature-dependent mobilities. Our simulations indicate that for PTB7-Th:PC$_{71}$BM solar cells, the temperature dependence of the carrier mobilities is critical in constructing the correct V_{OC} vs. T relation. It is important to investigate whether the V_{OC} vs. T relation of OSCs consisting of other state-of-the-art donor:acceptor materials can also be described using this method in the future as it can provide information about the dominant charge transport and recombination mechanisms in these devices.

Supplementary Material

See the supplementary material for details regarding the device fabrication, temperature-dependent characterization and analysis, and device energy level diagram.

References

[1] A. Karki, A.J. Gillett, R.H. Friend, and T.Q. Nguyen, "The Path to 20% Power Conversion Efficiencies in Nonfullerene Acceptor Organic Solar Cells," Adv Energy Mater **11**, 2003441 (2021).

[2] J. Luke, L. Corrêa, J. Rodrigues, J. Martins, M. Daboczi, D. Bagnis, and J.S. Kim, "A Commercial Benchmark: Light-Soaking Free, Fully Scalable, Large-Area Organic Solar Cells for Low-Light Applications," Adv Energy Mater **11**, 2003405 (2021).

[3] V. V. Brus, N. Schopp, S.J. Ko, J. Vollbrecht, J. Lee, A. Karki, G.C. Bazan, and T.Q. Nguyen, "Temperature and Light Modulated Open-Circuit Voltage in Nonfullerene Organic Solar Cells with Different Effective Bandgaps," Adv Energy Mater **11**, 2003091 (2021).

[4] G. Garcia-Belmonte, "Temperature dependence of open-circuit voltage in organic solar cells from generation–recombination kinetic balance," Solar Energy Materials and Solar Cells **94**, 2166–2169 (2010).

[5] W.J. Grzegorczyk, T.J. Savenije, T.E. Dykstra, J. Piris, J.M. Schins, and L.D.A. Siebbeles, "Temperature-Independent Charge Carrier Photogeneration in P3HT−PCBM Blends with Different Morphology," Journal of Physical Chemistry C **114**, 5182–5186 (2010).

[6] Y. Tang, J.M. Bjuggren, Z. Fei, M.R. Andersson, M. Heeney, and C.R. McNeill, "Origin of Open-Circuit Voltage Turnover in Organic Solar Cells at Low Temperature," Solar RRL **4**(11), 2000375 (2020).

[7] F. Gao, W. Tress, J. Wang, and O. Inganäs, "Temperature dependence of charge carrier generation in organic photovoltaics," Phys Rev Lett **114**, 128701 (2015).

[8] K. Vandewal, K. Tvingstedt, A. Gadisa, O. Inganäs, and J. V. Manca, "Relating the open-circuit voltage to interface molecular properties of donor:acceptor bulk heterojunction solar cells," Phys. Rev. B **81**, 125204 (2010).

[9] S.M. Menke, N.A. Ran, G.C. Bazan, and R.H. Friend, "Understanding Energy Loss in Organic Solar Cells: Toward a New Efficiency Regime," Joule **2**, 25–35 (2018).

[10] S. Xie, Y. Xia, Z. Zheng, X. Zhang, J. Yuan, H. Zhou, and Y. Zhang, "Effects of Nonradiative Losses at Charge Transfer States and Energetic Disorder on the Open-Circuit Voltage in Nonfullerene Organic Solar Cells," Adv Funct Mater **28**(5), (2018).

[11] J.C. Blakesley, and D. Neher, "Relationship between energetic disorder and open-circuit voltage in bulk heterojunction organic solar cells," Phys Rev B **84**, 075210 (2011).

[12] W. Yang, Y. Luo, P. Guo, H. Sun, and Y. Yao, "Leakage Current Induced by Energetic Disorder in Organic Bulk Heterojunction Solar Cells: Comprehending the Ultrahigh Loss of Open-Circuit Voltage at Low Temperatures," Phys Rev Appl **7**, 044017 (2017).

[13] H.H. Gullu, D.E. Yıldız, S.O. Hacioglu, A. Cirpan, and L. Toppare, "Dark conduction mechanisms of PTQBDT based heterojunction diode," Phys Scr **98**(1), 015819 (2022).

[14] M. Mingebach, C. Deibel, and V. Dyakonov, "Built-in potential and validity of the Mott-Schottky analysis in organic bulk heterojunction solar cells," Phys Rev B **84**, 153201 (2011).

[15] D. Rauh, A. Wagenpfahl, C. Deibel, and V. Dyakonov, "Relation of open circuit voltage to charge carrier density in organic bulk heterojunction solar cells," Appl Phys Lett **98**, 133301 (2011).

[16] Y. Liu, K. Zojer, B. Lassen, J. Kjelstrup-Hansen, H.G. Rubahn, and M. Madsen, "Role of the Charge-Transfer State in Reduced Langevin Recombination in Organic Solar Cells: A Theoretical Study," Journal of Physical Chemistry C **119**, 26588–26597 (2015).

[17] Z. Li, G. Lakhwani, N.C. Greenham, and C.R. McNeill, "Voltage-dependent photocurrent transients of PTB7:PC70BM solar cells: Experiment and numerical simulation," J Appl Phys **114**, 034502 (2013).

[18] L.J.A. Koster, V.D. Mihailetchi, and P.W.M. Blom, "Bimolecular recombination in polymer/fullerene bulk heterojunction solar cells," Appl Phys Lett **88**, 052104 (2006).

[19] G. Lakhwani, A. Rao, and R.H. Friend, "Bimolecular recombination in organic photovoltaics," Annu Rev Phys Chem **65**, 557–581 (2014).

[20] P. Zalar, M. Kuik, N.A. Ran, J.A. Love, T.-Q. Nguyen, P. Zalar, M. Kuik, N.A. Ran, J.A. Love, and T.-Q. Nguyen, "Effects of Processing Conditions on the Recombination Reduction in Small Molecule Bulk Heterojunction Solar Cells," Adv Energy Mater **4**, 1400438 (2014).

[21] G.J.A.H. Wetzelaer, N.J. Van Der Kaap, J.A. Koster, and P.W.M. Blom, "Quantifying Bimolecular Recombination in Organic Solar Cells in Steady State," Adv Energy Mater **3**, 1130–1134 (2013).

[22] C.R. McNeill, S. Westenhoff, C. Groves, R.H. Friend, and N.C. Greenham, "Influence of nanoscale phase separation on the charge generation dynamics and photovoltaic performance of conjugated polymer blends: Balancing charge generation and separation," Journal of Physical Chemistry C **111**, 19153–19160 (2007).

[23] P. Blom, M. de Jong, and M. van Munster, "Electric-field and temperature dependence of the hole mobility in poly(p-phenylene vinylene)," Phys Rev B **55**, R656 (1997).

[24] N.I. Craciun, J. Wildeman, and P.W.M. Blom, "Universal arrhenius temperature activated charge transport in diodes from disordered organic semiconductors," Phys Rev Lett **100**, 056601 (2008).

[25] N. Felekidis, A. Melianas, and M. Kemerink, "Automated open-source software for charge transport analysis in single-carrier organic semiconductor diodes," Org Electron **61**(March), 318–328 (2018).

[26] W.D. Gill, "Drift mobilities in amorphous charge-transfer complexes of trinitrofluorenone and poly-n-vinylcarbazole," J Appl Phys **43**(12), 5033 (2003).

[27] J.C. Blakesley, H.S. Clubb, and N.C. Greenham, "Temperature-dependent electron and hole transport in disordered semiconducting polymers: Analysis of energetic disorder," Phys Rev B **81**, 045210 (2010).

[28] M. Kuik, G.-J.A.H. Wetzelaer, H.T. Nicolai, N.I. Craciun, D.M. De Leeuw, P.W.M. Blom, N.I. Craciun, D.M. De Leeuw, W.M. Blom, M. Kuik, G.-J.A.H. Wetzelaer, and H.T. Nicolai, "25th Anniversary Article: Charge Transport and Recombination in Polymer Light-Emitting Diodes," Advanced Materials **26**, 512–531 (2014).

[29] R.P. Fornari, P.W.M. Blom, and A. Troisi, "How Many Parameters Actually Affect the Mobility of Conjugated Polymers?," Phys Rev Lett **118**, 086601 (2017).

[30] L.J.A. Koster, E.C.P. Smits, V.D. Mihailetchi, and P.W.M. Blom, "Device model for the operation of polymer/fullerene bulk heterojunction solar cells," Phys. Rev. B **72**, 085205 (2005).

[31] Y. Wu, Y. Li, B. van der Zee, W. Liu, A. Markina, H. Fan, H. Yang, C. Cui, Y. Li, P.W.M. Blom, D. Andrienko, and G.J.A.H. Wetzelaer, "Reduced bimolecular charge recombination in efficient organic solar cells comprising non-fullerene acceptors," Sci Rep **13**, 4717 (2023).

[32] L. Perdigón-Toro, L.Q. Phuong, F. Eller, G. Freychet, E. Saglamkaya, J.I. Khan, Q. Wei, S. Zeiske, D. Kroh, S. Wedler, A. Köhler, A. Armin, F. Laquai, E.M. Herzig, Y. Zou, S. Shoaee, and D. Neher, "Understanding the Role of Order in Y-Series Non-Fullerene Solar Cells to Realize High Open-Circuit Voltages," Adv Energy Mater **12**, 2103422 (2022).

[33] C.C.S. Chan, C. Ma, X. Zou, Z. Xing, G. Zhang, H.-L. Yip, R.A. Taylor, Y. He, K.S. Wong, and P.C.Y. Chow, "Quantification of Temperature-Dependent Charge Separation and Recombination Dynamics in Non-Fullerene Organic Photovoltaics," Adv Funct Mater **31**, 2107157 (2021).